Metastability and Uniqueness of Vortex States at Depinning

Mahesh Chandran,* R. T. Scalettar, and G. T. Zimányi
Department of Physics, University of California, Davis, California 95616
(Received 1 April 2002; published 10 October 2002)

We present results from numerical simulations of the transport of vortices in the zero-field-cooled (ZFC) and the field-cooled (FC) state of a type-II superconductor. In the absence of an applied current I, we find that the FC state has a lower defect density than the ZFC state, and is stable against thermal cycling. On the other hand, by cycling I, surprisingly, we find that the ZFC state is the stable state. The FC state is metastable as manifested by increasing I to the depinning current I_c, in which case the FC state evolves into the ZFC state. We also find that all configurations acquire a unique defect density at the depinning transition independent of the history of the initial states.

DOI: 10.1103/PhysRevLett.89.187001 PACS numbers: 74.60.Ge, 74.60.Jg

Metastability is a generic feature in many disordered systems. Metastable states show characteristics distinct from the ground state, and are evidenced, for example, by the path or history dependence of the different response functions. A striking example of metastability is the difference between the field-cooled (FC) and zero-field-cooled (ZFC) magnetization in the vortex phase of type-II superconductors [1]. In superconductors, the FC magnetization is much smaller than the ZFC magnetization. This difference decreases with increasing temperature T and vanishes above the irreversibility temperature $T_{\rm irr}$. The ZFC state is believed to be metastable and the FC state to be a quasiequilibrium state because it is possible to reach the FC state from the ZFC state by changing T from a low value to $T_{\rm irr}$ and back, but the ZFC state cannot be reached from a FC state through such a temperature cycle. Similar features are also observed in spin glasses [2]. The difference in FC and ZFC state magnetization is explained by the emergence of energy barriers below $T_{\rm irr}$, which inhibits the ZFC state from exploring the full configuration space.

In recent years, transport experiments have shown conflicting results regarding the stability of the FC and the ZFC states. In the anomalous peak effect region, the FC state has been observed to be unstable against current annealing. The critical current I_c is higher (up to a factor of 6) in the virgin FC state than in FC states annealed by a current or in the ZFC state [3]. On the other hand, using a slow ramp rate for I, the FC and ZFC state I_c was found to be the same below and inside the peak effect regime [4]. This was interpreted as a signature of the metastability of the FC state. Also, the susceptibility of the FC state can be switched to that of the ZFC state by applying an ac pulse [5,6]. Moreover, recent scanning Hall probe measurements have also shown substantial vortex rearrangement in FC states for $I < I_c$ [7]. One approach accounts for these experimental observations through the role of surface barriers [8]. These differing pictures place in the focus the behavior of vortices in the FC and ZFC states in the presence of a transport current.

In this paper, we use numerical simulations to study the transport of differently prepared vortex systems. Our first main result is that, in contrast to the temperature cycling, if the vortex system is cycled with a transport current, then the ZFC state is more stable than the FC state. In particular, the ZFC state can be reached from the FC state by current cycling, but not vice versa. Our second main result is that, with increasing currents, all vortex states, FC, ZFC, or prepared in any intermediate way, acquire a *unique density of defects at depinning*.

We consider vortices in a 2D plane perpendicular to the magnetic field $\mathbf{B} = B\hat{\mathbf{z}}$ of a bulk superconductor, with $B = n_v\phi_0$, where n_v is the vortex density, and ϕ_0 is the flux quantum. Within the London approximation, we treat the vortices as particles, with dynamics governed by an overdamped equation of motion,

$$\eta\frac{d\mathbf{r}_i}{dt} = -\sum_{j\neq i}\nabla U^v(\mathbf{r}_i - \mathbf{r}_j) - \sum_k \nabla U^p(\mathbf{r}_i - \mathbf{R}_k) + \mathbf{F}_{\rm ext} + \boldsymbol{\zeta}_i(t).$$

Here, η is the flux-flow viscosity, and the first term represents the intervortex interaction given by the potential $U^v(r) = [\phi_0^2/(8\pi^2\lambda^2)]K_0(\tilde{r}/\lambda)$, where K_0 is the zeroth-order Bessel function, and $\tilde{r} = (r^2 + 2\xi^2)^{1/2}$ with λ and ξ as penetration depth and coherence length of the superconductor, respectively [9]. The second term is the attractive interaction with parabolic potential wells $U^p(r) = U_0[(r^2/r_p^2) - 1]$ for $r < r_p$, and 0 otherwise, centered at the random $\mathbf{R}_k$ locations. The third term $F_{\rm ext} = \frac{1}{c}\mathbf{J}\times\phi_0\hat{\mathbf{z}}$ represents the Lorentz force due to the transport current density $\mathbf{J}$. The last term is the thermal noise (Langevin term) with the moments $\langle\zeta_{i,p}(t)\rangle = 0$, and $\langle\zeta_{i,p}(t)\zeta_{j,p'}(t')\rangle = 2k_BT\eta\delta_{ij}\delta_{pp'}\delta(t-t')$, where T is the temperature, k_B is the Boltzmann constant, and $p, p' = x, y$. We worked with reduced variables: All distances are in units of $\lambda_0 = \lambda(T=0)$, the current density J in units of cf_0/ϕ_0, and T in units of $\lambda_0 f_0/k_B$, where $f_0 = \phi_0^2/(8\pi^2\lambda_0^3)$. The time t is in units of $\eta\lambda_0/f_0$. This model is expected to reasonably capture the physics of

stiff vortex lines, such as those in Nb and $NbSe_2$, while in strongly layered superconductors, the soft interlayer couplings introduce additional degrees of freedom.

To simulate the ZFC state, we confine the quenched disorder to a central region of the simulation box, while leaving the outer region defect-free as illustrated in Fig. 1. The disordered region defines the extent of the superconductor and the disorder-free region simulates the free space. Periodic boundary conditions connect the edges of the simulation box. We employ a box of size $40\lambda_0 \times 24\lambda_0$, with the disordered region occupying $28\lambda_0 \times 24\lambda_0$. We used a pin density of $5.95/\lambda_0^2$ with $\langle U_0 \rangle = 0.03$ and $r_p = 0.1\lambda_0$. The results presented below are for $N_v = 1148$ vortices in the simulation box which corresponds to $B \approx 800$ G. Typically, we used 5×10^4 time steps for thermal equilibration. For V-I characteristics, 2×10^4 time steps were used to equilibrate before averaging over a similar time scale. The real space configuration of vortices is characterized by the defect density $n_d = N_d/S$, where N_d is the number of vortices which are nonsixfold coordinated and S is the area (in units of λ_0^2) of the disordered region [10]. N_d is counted by Delaunay triangulation of the real space position of vortices. The V-I characteristics are calculated by varying $\mathbf{F}_{\rm ext} = F_{\rm ext}\hat{\mathbf{x}}$ ($F_{\rm ext} \propto I$, the current) and calculating the average velocity ($\propto V$, the voltage) $\mathbf{v} = (1/N_v)\sum_i^{N_v} \dot{\mathbf{r}}_i$ along the x axis.

We first consider the effect of cycling the temperature T. The ZFC state at $T = 0$ is created by positioning vortices in the defect-free region and allowing them to move into the disordered region by their own dynamics. The FC state is created by the thermal cycle of the ZFC state by first heating the system deep into the liquid phase, and, subsequently, cooling it back to $T = 0$. Figure 1 shows the behavior of the defect density n_d throughout this thermal cycle. The ZFC state at $T = 0$ is formed by vortices diffusing through the free edges into the disordered region. With decreasing velocity of the diffusion front, plastic deformation induces a larger density of defects. These defects are nonequilibrium and are supported by a gradient ($\propto \langle U^p \rangle$) in vortex density [11]. On increasing T, the gradient, and, subsequently, $n_d(T)$, decreases due to thermal activation. Across $T = 0.012 = T_m$, the melting temperature, $n_d(T)$ increases rapidly as the system goes into the liquid phase. Compared to the ZFC state, the FC state has a lower $n_d(T = 0)$ as it is cooled from the homogeneous liquid phase that has no macroscopic density gradients. The FC state shows no appreciable change in n_d on repeated thermal cycling. The inset of Fig. 1 shows the hysteresis in n_d on crossing T_m, which is evidence for the melting transition into the liquid phase being first order. A very slow cooling rate is used in the inset compared to the main panel to more accurately observe the hysteresis across T_m.

A partial thermal cycling of the system, consisting of a warming step to a temperature $T_{\rm PFC}$, e.g., $T_{\rm PFC} = 0.006 = T_m/2$, and a subsequent cooling step to $T = 0$ generates a

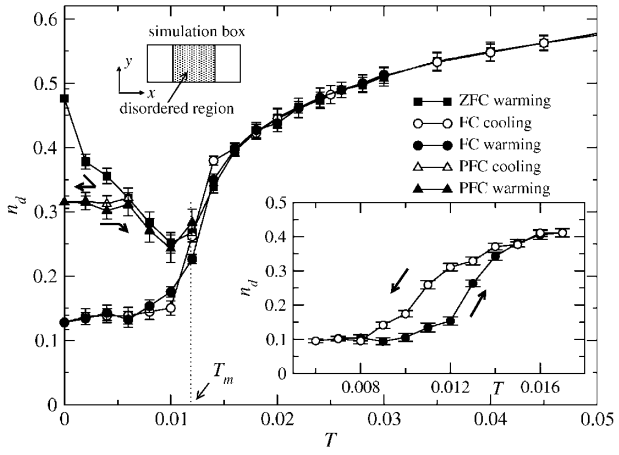

FIG. 1. Plot of $n_d(T)$ for the thermal cycling starting with the ZFC state at $T = 0$. Also shown is the partial stability of the PFC state, created by cooling from $T_{\rm PFC} = 0.006$. The direction in which T is changed for creating the PFC state is shown by thick arrows. The simulation geometry is shown on the upper left corner of the main panel. Inset: hysteresis in n_d across T_m during the FC cooling and warming procedure.

partially field-cooled (PFC) state (see Fig. 1). The PFC state is less disordered than the ZFC state, and is stable to thermal cycling between 0 and $T_{\rm PFC}$. For $T > T_{\rm PFC}$, the PFC state follows the same path as the virgin ZFC state. This repeated warming and cooling allows one to access all the other PFC configurations at $T = 0$. The behavior of $n_d(T)$ is in consonance with the experimental measurement of magnetization $M(T)$ for $T < T_{\rm irr}$ [1].

Next, we consider the effect of current I on various configurations. As shown in Ref. [12], effects of the disorder on the moving vortex state can be characterized by a "shaking temperature" T_{sh}. $T_{sh} \propto v^{-1}$, where $v \propto I$ is the average vortex velocity. At large v, a moving lattice is formed which undergoes an order to disorder transition as I is decreased to zero across the depinning current I_c. Therefore, besides the above described thermal cycling, a disordered vortex state can be prepared by current cycling as well. As will be shown below, the resulting configuration is the most stable vortex state against repeated cycling of I. We call the resulting static configuration the current hardened (CH) state, in analogy to "strain hardening," in which materials are cycled with increasing stress to increase the density of dislocations.

Figure 2 shows $V(I)$ and $n_d(I)$ curves at $T = 0$ for differently prepared states. We identify three current regimes: (i) a pinned regime $I < I_c$, with $V = 0$ and $n_d(I)$ determined by the mode of preparation; (ii) a plastic regime $I_c < I < I_m$, with nonlinear $V(I)$ and the *same* $n_d(I)$ for all differently prepared states; and (iii) a flowing-lattice regime $I > I_m$, with linear $V(I)$ and $n_d(I)$ substantially smaller. The small difference in n_d in the flowing-lattice regime, as seen in Fig. 2, is due to the formation of a grain boundary at the free edges of the

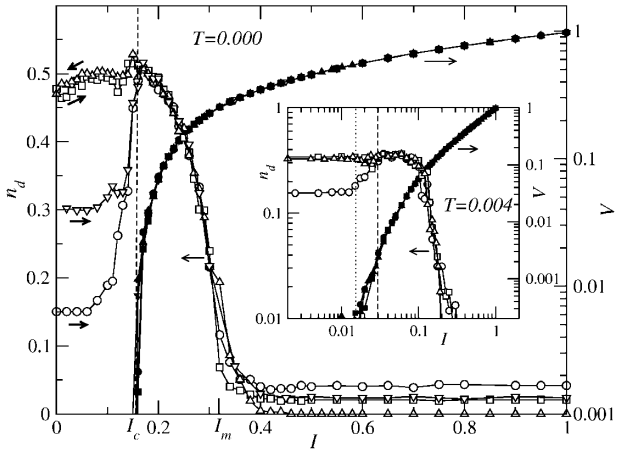

FIG. 2. $V(I)$ (solid symbols), and $n_d(I)$ (open symbols) at $T = 0$ for the FC state (∘), PFC state (▽), ZFC state (□), and CH state (△). The direction in which current is changed is shown by thick arrows. Inset: same as the main panel for $T = 0.004$. The dashed and the dotted lines mark $I_{\rm irr}$ and I_c, respectively.

disorder region [see also Fig. 4(c)]. Remarkably, $V(I)$ curves and the depinning current I_c are independent of the mode of preparation of the system [13], in agreement with the experiments with slow ramping of I [4]. These characteristics persist at finite T as well. The $n_d(I)$ for $I < I_c$, on the other hand, depends on the mode of preparation.

Strikingly, the defect density $n_d(I)$ at the depinning current I_c assumes the *same* value $n_d^c \approx 0.51$ for the FC, ZFC, PFC, and CH states, as seen in Fig. 2. In other words, n_d^c is *independent of the mode of the preparation of the vortex state.* The history independent unique value of n_d^c implies that the characteristics and dynamics of all vortex states converge as the current approaches I_c. This idea is substantiated by studying the real space dynamics at depinning. As is known, vortices depin by forming a few channels across the system [14]. We find that, while in differently prepared states the channels are nucleated at different locations along the entry edge, in the bulk the channels converge quickly to a universal pattern. We also find the average transverse wandering of a channel is of the order of ~6–7 lattice constants, and is the same for all states at I_c. This implies that the average displacement of the vortices at I_c is the same for all states, thus providing an underlying physical picture for preparation independence of n_d^c. Further studies show that the value of n_d^c depends on T, n_v, and the disorder strength.

Next, we study the stability of the different vortex states against cycling with I. The virgin FC state has a defect density $n_{d,\rm FC}(0) < n_d^c$. Therefore, the density of defects in the virgin FC state increases from $n_{d,\rm FC}(0)$ to n_d^c as the I is increased from 0 to I_c, as shown in Fig. 2. Furthermore, decreasing current from $I_1 < I_c$, $n_{d,\rm FC}(I)$ does not decrease to its virgin value, but stays approximately at $n_d(I_1)$. In particular, cycling I between 0 and $I \geq I_c$ leaves $n_{d,\rm FC}(I) \approx n_d^c$ for $I < I_c$. At the same time, $n_{d,\rm ZFC}(0) \approx n_d^c$, and cycling I does not affect this value. Therefore, the FC state, and its defect density $n_{d,\rm FC}$, can be transformed into the ZFC state and $n_{d,\rm ZFC}$ by cycling I between 0 and I_c. The reverse is not true, i.e., *the FC state cannot be reached from any state by cycling current.* Therefore, in contrast to thermal cycling, we find that the FC state is metastable and the ZFC state is stable against current cycling. Figure 2 further illustrates that the CH state and its defect density $n_{d,\rm CH}(I)$ evolve into the ZFC state when the current is decreased from a large value to 0. The same holds for the PFC states, as $n_{d,\rm PFC}(I)$ also evolves into $n_{d,\rm ZFC}(0)$.

Since for $I > I_c$ $n_d(I)$ is approximately the same for all states, metastable configurations and the irreversible behavior of $n_d(I)$ emerge only below $I_{\rm irr}$. For $T = 0$, $I_{\rm irr} = I_c$, but at finite temperatures these two current values separate, as evident for $T = 0.004$, shown in the inset of Fig. 2. At finite T, $n_d(I) \approx n_d^c$ at a current $I_{\rm irr} > I_c$. This is possibly due to thermally activated vortex creep, which induces vortex displacements already for $I < I_{\rm irr}$. The metastability of the FC state persists at finite T, and we believe is a generic phenomenon which brings out a fundamental difference in the nature of FC and ZFC states. The ZFC and CH states show similar behavior throughout the studied current and temperature ranges.

Further evidence for metastability of the FC state is obtained by applying a current pulse $I = 0.15 < I_c$ to differently prepared vortex states, and observing the temporal evolution of n_d, as illustrated in Fig. 3(a). The application of a current pulse evolves the FC state into PFC states with an intermediate defect density $n_{d,\rm FC} < n_{d,\rm PFC} < n_{d,\rm ZFC}$. The defect density remains at that elevated level even after the current drops to zero. In particular, a large enough current pulse evolves the FC state

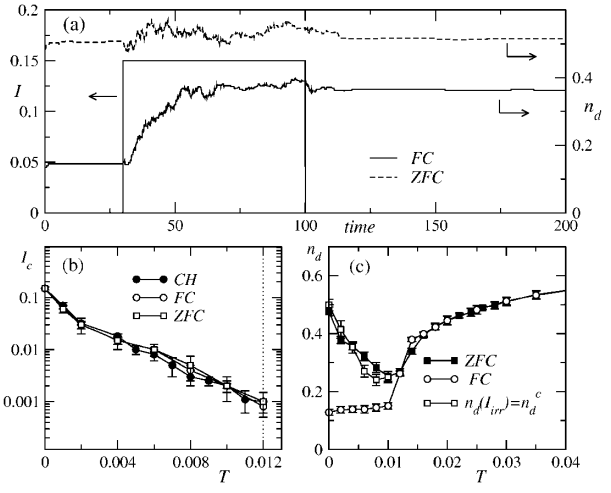

FIG. 3. (a) The time evolution of n_d at $T = 0.0$ for a pulse of current $I = 0.15 < I_c$ in the ZFC and the FC state. (b) Plot of $I_c(T)$ obtained from FC, ZFC, and CH states. (c) $n_d^c(T)$ obtained from $V(I)$ curves along with n_d for ZFC warming and FC cooling superimposed from Fig. 1.

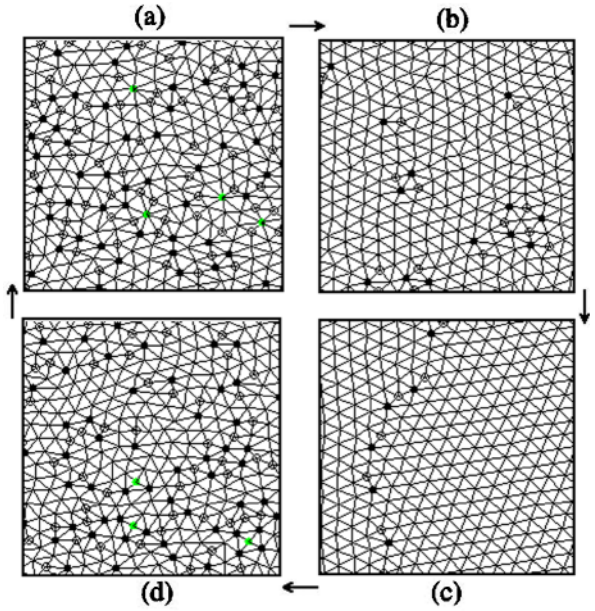

FIG. 4 (color online). The real space configuration at $T = 0$ during a composite T-I cycle: (a) ZFC state, (b) FC state, (c) flowing lattice state, (d) CH state. The arrows show the cycling path (see text for details). Note the close similarity between (a) and (d). The symbols (∘) and (•) denote vortices with five and seven neighbors, respectively.

into the ZFC state. This transformation of the FC state to the ZFC state by a current pulse is in close analogy to experimental observations [5]. In Ref. [5], the I_c is also found to change during the transformation of the FC state to the ZFC state, possibly due to the influence of the surface barrier [15]. We emphasize that the transformation of the FC configuration to ZFC configuration as found here is a bulk characteristic, and is not influenced by the free edges of the disordered region. This was verified in simulation without free edges [16]. The FC state was again found to be metastable below $I_{\rm irr}$, and is transformed into CH configuration on increasing I above $I_{\rm irr}$.

In Fig. 3(b), we plot $I_c(T)$ for a range of T at which simulations were carried out. The I_c follows an $\exp(-\frac{T}{T_0})$ form, confirming that thermally activated motion dominates the dynamics at I_c. Figure 3(c) shows the temperature dependence of $n_d^c(T)$, as obtained from $V(I)$ curves. The $n_d(T)$ values for the FC and ZFC states are superimposed from Fig. 1. $n_d^c(T)$ closely follows $n_{d,\rm ZFC}(T)$, obtained by warming the ZFC state, thus corroborating the view that the ZFC state is essentially the frozen equivalent of the critical state at I_c. In other words, the channels formed by the penetrating front of vortices during the formation of the virgin ZFC state is frozen. Any subsequent application of I essentially uses these preformed channels which explains why the ZFC state shows no substantial change in n_d. In contrast, in the virgin FC state no such channels exists. On first passage of I, the resulting buildup of stress at depinning leads to channel formation which increases n_d. Any further cycling of I essentially uses the already formed channels. This is a plausible explanation for the metastability of the FC state on cycling I.

The configurational changes are illustrated in Fig. 4 for various states, during a composite T-I cycle. Starting with the ZFC state, shown in Fig. 4(a), we obtain the FC state [Fig. 4(b)] by cycling T from 0 to $T > T_m$. The FC state is then driven with $I > I_m$ to obtain Fig. 4(c). Finally, decreasing I to 0, the CH state is obtained in Fig. 4(d), which is indistinguishable from the ZFC state in Fig. 4(a). *Thus, a composite T-I cycle allows one to go from the ZFC state to the FC state and vice versa.*

In conclusion, we have shown that the ZFC state is stable against current cycling in contrast to the FC state which is found to be metastable. This behavior is opposite to the thermal cycling where the FC state is stable. We also find that the defect density n_d for any initial state converges to the same value at I_c.

We thank Helmut Katzgraber for critical reading of the manuscript. M. C. also acknowledges useful discussions with E. Zeldov and A. K. Grover during the course of the work. This work was supported by NSF-DMR 9985978.

*Electronic address: chandran@physics.ucdavis.edu

[1] K. A. Müller *et al.*, Phys. Rev. Lett. **58**, 1143 (1987).
[2] K. Binder and A. P. Young, Rev. Mod. Phys. **58**, 801 (1986); K. H. Fischer and J. A. Hertz, *Spin Glasses* (Cambridge University, Cambridge, England, 1991).
[3] W. Henderson *et al.*, Phys. Rev. Lett. **77**, 2077 (1996).
[4] Z. L. Xiao *et al.*, Phys. Rev. Lett. **85**, 3265 (2000).
[5] S. S. Banerjee *et al.*, Appl. Phys. Lett. **74**, 126 (1999).
[6] S. O. Valenzuela and V. Bekeris, Phys. Rev. Lett. **86**, 504 (2001).
[7] M. Marchevsky, M. J. Higgins, and S. Bhattacharya, Phys. Rev. Lett. **88**, 087002 (2002).
[8] Y. Paltiel *et al.*, Nature (London) **403**, 398 (2000).
[9] J. R. Clem, J. Low Temp. Phys. **18**, 427 (1975).
[10] We choose to define defect density rather than defect fraction because the number of vortices within the disordered region is not fixed but fluctuates with time.
[11] C. P. Bean, Phys. Rev. Lett. **8**, 250 (1962).
[12] A. E. Koshelev, and V. M. Vinokur, Phys. Rev. Lett. **73**, 3580 (1994).
[13] We find different I_c on repeated current cycling due to metastable states present during plastic depinning. But the distribution width of I_c is the same for any starting configuration, viz. FC, ZFC, PFC, and CH, and is not more than 2% of the average I_c.
[14] K. Moon *et al.*, Phys. Rev. Lett. **77**, 2778 (1996); N. Grønbech-Jensen *et al.*, Phys. Rev. Lett. **76**, 2985 (1996); S. Ryu *et al.*, Phys. Rev. Lett. **77**, 5114 (1996); C. J. Olson *et al.*, Phys. Rev. Lett. **80**, 2197 (1998); H. Fangohr *et al.*, Phys. Rev. B **64**, 064505 (2001).
[15] Z. L. Xiao *et al.*, Phys. Rev. B **65**, 094511 (2002).
[16] Since the ZFC state cannot be simulated without free edges, we compared only the FC and the CH states.